Allogeneic mesenchymal stem cells and xenogenic platelet rich plasma, associated or not, in the repair of bone failures in rabbits with secondary osteoporosis[1]

Mariá Andrade de Carvalho Rocha[I], Laís Meireles Costa Silva[I], Wellson Andrade de Oliveira[I], Dayseanny de Oliveira Bezerra[II], Gustavo Cardoso da Silva[III], Lucilene dos Santos Silva[IV], Brenda Lurian do Nascimento Medeiros[V], Sílvia de Araújo França Baêta[VI], Maria Acelina Martins de Carvalho[VII], Napoleão Martins Argôlo Neto[VIII]

[I]Fellow Master degree, Postgraduate Program in Animal Science, Universidade Federal do Piauí (UFPI), Teresina-PI, Brazil. Radiography, technical procedures, obtaining platelet-rich plasma.
[II]Fellow PhD degree, Postgraduate Program in Animal Science, UFPI, Teresina-PI, Brazil. Anesthetic, technical procedures.
[III]Fellow PhD degree, Northeast Network of Biotechnology, UFPI, Teresina-PI, Brazil. Computerized image analysis.
[IV]Fellow Postdoctoral degree, National Postdoctoral Program (PNPD/CNPq), UFPI, Teresina-PI, Brazil. Photomicrographs and histopathological examinations.
[V]Graduate student, UFPI, Teresina-PI, Brazil. Technical procedures.
[VI]PhD, Associate Professor, Department of Clinical and Veterinary Surgery, UFPI, Teresina-PI, Brazil. Histopathological examinations, supervised all phases of the study.
[VII]PhD, Associate Professor, Department of Veterinary Morphology, UFPI, Teresina-PI, Brazil. Bioethical supervision.
[VIII]PhD, Associate Professor, Department of Clinical and Veterinary Surgery, UFPI, Teresina-PI, Brazil. Design of the study, supervised all phases of the study.

Abstract

Purpose: To assess the efficacy of allogeneic mesenchymal stem cells and xenogenic platelet rich plasma in the treatment of bone failure of osteoporotic rabbits secondary to estrogenic deprivation and iatrogenic hypercortisolism.

Methods: Eight female rabbits underwent ovarian resection and corticoid therapy to induce clinical status of osteoporosis. Four failures were produced in the tibiae, with each failure being treated with hemostatic sponge, allogenic mesenchymal stem cells, xenogenic platelet-rich plasma and the association between both. The animals were divided into two groups, evaluated radiographically and histopathologically at 30 and 60 days post treatment.

Results: A radiographically confirmed consolidation of bone failures treated with allogeneic mesenchymal stem cells, associated with the histopathological image of mature and immature bone tissue, without evidence of osteopenia, was compared with the other groups, in which radiolucent failures with osteopenia and fibrosis were still present, denoting the satisfactory effect of the first treatment in detriment to the others.

Conclusion: The treatment of bone failures of rabbits with secondary osteoporosis with allogeneic mesenchymal stem cells induced greater bone consolidation with mature and immature bone tissue production ($p<0.01$), when compared to the other treatments.

Key words: Mesenchymal Stromal Cells. Platelet-Rich Plasma. Osteoporosis. Rabbits.

■ Introduction

Osteoporosis is a systemic bone disease characterized by a marked reduction of mineral mass, decreasing the mechanical strength of the bone and increasing the risk of fractures[1]. Several mechanisms are recognized as predisposing and perpetuating factors of osteopenia induced by osteoporosis, including endocrine and pharmacological factors[2].

Chronic iatrogenic hypercortisolism is the most frequent cause of secondary osteoporosis, corresponding to 25% of the etiologies in humans[3]. According to these authors, glucocorticoids can induce parathyroid hyperplasia, with subsequent serum increase in parathyroid hormone levels (PTH), stimulating calcium reabsorption and release of calcium and phosphorus ions into the extracellular environment[4].

In contrast, estrogen and its analogues have a prophylactic effect on bone resorption, acting as modulators of remodeling of this tissue[2,5]. This effect results from autocrine and paracrine control over the expression of growth factors and cytokines that influence the behavior of osteoblasts and osteoclasts, contributing to the maintenance of the functional bone balance[5].

According to Amadei *et al.*[5], in Brazil, each year, 70.000 people suffer from osteoporotic fractures, with rates of 20% of mortality and 50% of physical disability. Costs for the Unified Health System with the hospitalization of these patients were estimated at approximately R$ 908.18 per capita[6].

Currently, bisphosphonates are the most effective drugs for the treatment of human osteoporosis. However, adverse effects such as gastrointestinal intolerance[7], esophageal erosions, fever, atrial fibrillation, scleritis and mandibular osteonecrosis[7] have been described, limiting its wide use[8].

The use of mesenchymal stem cells (MSC) for the treatment of bone fractures has been highlighted as an innovative proposal, due to the high plasticity of these cells and the demonstration of in vitro differentiation capacity in osteoblasts[9,10]. Previous studies have already demonstrated the efficacy of MSC in the consolidation of fractures in healthy or non-healthy patients[11,13].

In addition to this alternative, autogenous platelet-rich plasma (PRP) has been used in contemporary studies with human and animal patients to stimulate bone repair[12,13]. This compound is rich in growth factors that stimulate mitogenesis, angiogenesis and increased activity of osteocompetent cells, determining rapid formation and bone homogeneity[13]. It presents low yield, by volume, from the initial blood sample, which limits its use in small species[14]. In addition, studies with xenogeneic PRP are scarce and its real effect on bone remodeling is unknown.

Moreover, according to Amadei *et al.*[5], the clinical experience regarding bone repair in osteoporosis is inconsistent, due to few studies performed on the subject.

The objective of this study was to evaluate the effect of the treatments with hemostatic sponge of hydrolyzed collagen, medullary allogeneic MSC, equine xenogeneic PRP and the association between both, in the repair of bone failures in tibiae of osteoporotic rabbits secondary to estrogenic deprivation and iatrogenic hypercortisolism.

■ Methods

The experimental design was approved by the Animal Experimentation Ethics Committee (CEEA) of Federal University of Piauí (UFPI), according to the standards of the Brazilian College of Animal Experimentation (COBEA).

Eight rabbits (*Oryctolagus cuniculus*), New Zealand breed, female, nulliparous, one year old and average weight of 2.1 ± 0.19 kg were used. Clinically healthy rabbits (normophagia, normoquezia, normodipsia

and normouria) were selected and presented hematological evaluation and serum urea and creatinine values within the normal range for the specie[17]. The animals were submitted to a 10-day acclimation period and managed in a confinement system according to the welfare practices for the species.

Evaluation of serum calcium and phosphorus

All animals were fasted for six hours and sedated with a combination of ketamine (50 mg/kg) and midazolam (10 mg/kg) by intramuscular route in the femoral quadriceps, for blood collecting by jugular vein puncture for measurements serum calcium ionizable and serum phosphorus.

Calcium and phosphorus measurements were performed by colorimetric spectrophotometry, measured once, before ovariosalpingohysterectomy (OSH) elective and induction of hypercortisolism and once at 80 and 60 days thereafter, respectively.

Induction of osteoporosis

All animals were submitted to ovariosalpingohysterectomy elective, as described by Bueno *et al*.[15]. After 60 days, the induction of hypercortisolism was initiated through the administration of methylprednisolone succinate, as described by Rocha *et al*.[19].

Radiographic optic densitometric evaluation

All animals were submitted to radiographic optical densitometric examination using an 11-step ultra-purified aluminum penetrometer and the images obtined were analyzed by Adobe Photoshop CC 64-Bit software, before and after osteoporosis induction, as described by Rocha *et al*.[19]. All radiographic images were performed in the Diagnostic Imaging Sector of the University Veterinary Hospital, UFPI.

Obtaining of allogeneic mesenchymal stem cells

The MSC were donated by the Integrated Nucleus of Morphology and Research with Stem Cell (NUPCelt /UFPI). The cells were isolated from the bone marrow of healthy, expanded in vitro rabbits submitted to osteogenic and chondrogenic cell differentiation assay and aliquoted at the concentration of $1x10^6$ cells/mL for immediate use, according to methodologies previously described by Argolo Neto *et al*.[9,16] and Carvalho *et al*.[10].

Evaluation of the interaction between mesenchymal stem cells and hemostatic sponge of hydrolyzed collagen

Three aliquots of $1x10^4$ MSC were maintained in complete F12 DMEM medium, together with a 3 mm sample of sterile hemostatic sponge of hydrolyzed collagen, in a six-well culture plate, incubated at 37°C, 5% CO_2 and 95% moisture[16].

After obtaining confluence of 80%, the hemostatic sponge fragment was removed, washed with buffered phosphate solution and the MSC were trypsinized and evaluated for cell viability as described by Argolo Neto *et al*.[9].

The fragments of the hemostatic sponge were fixed isolated in 5% formaldehyde alone for 24 hours, dehydrated in increasing concentrations of alcohol (30%, 55%, 70%, 88%, 96%), diaphanized in xylol, included in histological paraffin and sectioned on rotary microtome, adjusted to 4µm thickness. The cuts were fixed on a glass slide, stained by Hematoxylin & Eosin and analyzed in a binocular optical microscope in x20 and x40 objective.

Obtaining xenogenic platelet rich plasma

Blood of a clinically healthy, dewormed equine was used, hematimetric values within the normal range for the specie[17] and total

platelet count of $200x10^3/mm^3$ or greater. Blood was immediately processed according to the methodology described by Del Carlo *et al*.[12] and Argolo Neto *et al*.[16] and the PRP prepared immediately before application.

Experimental design

A design was adopted a 30-day and 60-day (four animals each) post-surgical observation period and four experimental groups (MSC, PRP, association between MSC and PRP-ASSO and control-CTR) were used. All groups coexisted in each animal, totalizing eight bone failures for each treatment. Two failures occurred in the diaphysis of the right and left tibia, in a third most proximal to the epiphyses, in all the animals. MSC treatments were standardized on superior bone failure of the right pelvic limb tibia, PRP on lower tibial bone failure of the right pelvic limb, ASSO on superior bone failure of the left pelvic limb tibia and CTR on lower tibial bone failure of the left pelvic limb.

Production of bone failures

All animals were submitted to antibiotic therapy with enrofloxacin (10 mg/kg) by intramuscular route and analgesia for administration of morphine (5 mg/kg) by intramuscular route in the pre, trans and postoperative, during ten and five days, respectively. After 2 hours of water fasting and feeding of 6 hours, anesthesia was induced by the association of ketamine (50 mg/kg) and midazolam (10 mg/kg) by intramuscular route in the femoral quadriceps, followed by intubation and anesthetic maintenance with 2% isoflurane.

The surgical field was delimited by a fenestrated field and a longitudinal incision of the skin was performed using scalpel n.3 with a n.15 blade, divulsing the subcutaneous tissue, fascia lata and cranial tibial muscle with a blunt surgical scissors, until bone exposure. Then, with an orthopedic drill equipped with a 2 mm steel drill and a drill guide[10], at a speed of 5000 rpm, bone failures of 2 mm in diameter were performed, with two failures in the proximal superior and inferior diaphyseal region of the right tibia and two failures in the proximal superior and inferior diaphyseal region of the left tibia, perpendicular to the bone diaphysis.

After the immediate realization of the treatments, the cranial tibial muscle divulsioned fibers were closed in the Sultan interrupted suture plane and the skin with single interrupted suture, both using 3-0 nylon monofilament yarn.

The animals were maintained with the use of elizabethan collar continuous and the surgical wounds were cleaned daily with sterile saline solution and topical application of allantoin and chlorhexidine ointment.

Conducting treatments

The bone failures were treated immediately, according to the experimental group they composed. All treatments were performed using 3 mm fragments of sterile hydrolyzed collagen hemostatic (EH) sponge, as structural support (*scaffold*) for MSC and / or PRP, introduced in the failures. The MSC group was treated with $1x10^6$ cells on EH, the PRP group with $1x10^6$ platelets on EH, the ASSO group with the association between MSC and PRP on EH at the same concentrations and CTR only with EH embedded in sterile physiological solution.

Radiographic optical densitometry of bone failures

After 30 and 60 days of the realization of treatments, the bone failures of all the animals were submitted to the radiographic optical densitometric examination.

Histopathological evaluation of tibial bone failures

After 30 and 60 days of the realization of treatment, four animals were sedated,

respectively, by the association with midazolam and ketamine, and euthanized with anesthetic overdose of thiopental sodium (30mg/mL) given intravenously.

Surgical amputation of the right and left tibias of all rabbits was performed. Each failure of each tibia was sectioned with the aid of a surgical electric saw keeping two centimeters of bone above and below the failures, identified and preserved individually in 10% buffered formaldehyde.

The bone fragments were decalcified in a solution containing 20% sodium citrate and 50% formic acid in 1: 1 dilution in distilled water.

The decalcified fragments were routinely processed, included in histological paraffin[9], sectioned in a rotating microtome[10], adjusted to 5µm thickness, stained by Hematoxylin & Eosin and analyzed in binocular optical microscope in x10 and x20 objective.

Statistical analysis

Values of 10 to 30, on a scale of 10, were arbitrarily assigned, corresponding to the radiographic optical density intervals, in cm^3, of each bone failure evaluated, according to Table 1.

Table 1 - Scores arbitrarily adopted to correspond to the intervals measured, in cm^3, of radiographic optical densitometry of tibial bone failures of rabbits at 30 and 60 days post treatment.

Interval (cm^3)	Score
0 – 1.37	0
1.37 – 1.40	10
1.41 – 1.44	20
1.44 – 1.47	30

Statistical analysis was performed with Bioestat® software v. 5.9, applying the Kruskal-Wallis non-parametric analysis of independent samples, followed by the Dunn station median comparison test, adopting a level of rejection of the null hypothesis of 1% ($p \leq 0.01$) for both analyzes.

■ Results

An average serum elevation of 2.54±1.21 mg/dL of ionizable calcium and 1.23±0.99 mg/dL of phosphorus was observed after induction of iatrogenic hypercortisolism and osteoporosis (Table 2). Only two animals had a reduction in serum ionizable calcium levels and three in serum phosphorus after the experimental induction period.

Table 2 - Serum values of ionizable calcium and phosphorus of adult nulliparous rabbits, submitted to ovariosalpingohysterectomy, before and after induction of iatrogenic hypercortisolism and osteoporosis.

	Serum ionizable calcium (mg/dL)		Serum phosphorus (mg/dL)	
	Before induction	After induction	Before induction	After induction
Animal 1	12.10	16.20$^+$	3.60	6.40$^+$
Animal 2	10.90	12.10$^+$	5.30	5.40$^+$
Animal 3	11.20	13.20$^+$	4.90	5.90$^+$
Animal 4	12.80	11.90$^-$	5.60	4.40$^-$
Animal 5	10.50	14.50$^+$	3.70	4.60$^+$
Animal 6	11.90	14.00$^+$	5.00	4.40$^-$
Animal 7	12.30	11.40$^-$	6.20	4.00$^-$
Animal 8	12.30	14.16$^+$	4.55	5.92$^+$
Average	**11.75±0.74**	**13.43±1.50**	**4.86±0.89**	**5.13±0.89**
Average increase	**2.54±1.21**		**1.23±0.99**	

$^+$Animals that presented elevation of serum levels; $^-$Animals that presented decrease of serum levels.

The radiographic optical densitometry of the tibiae of the rabbits before the induction of iatrogenic hypercortisolism and osteoporosis, identified values above 1.375 cm³ and below 1.465 cm³. The graph in red indicates that the bone mineral density of the tibia is located between the densities of the penetrometer steps. Comparing the bone density between the same rabbits, perceive the decrease bone density in red at levels lower than 1.375 cm³ after induction of the model (Figure 1, Table 3).

It was not possible to measure the precise decay value of the optical bone density after induction of the model, because the density observed was lower than the last lower step, of lower density of the penetrometer.

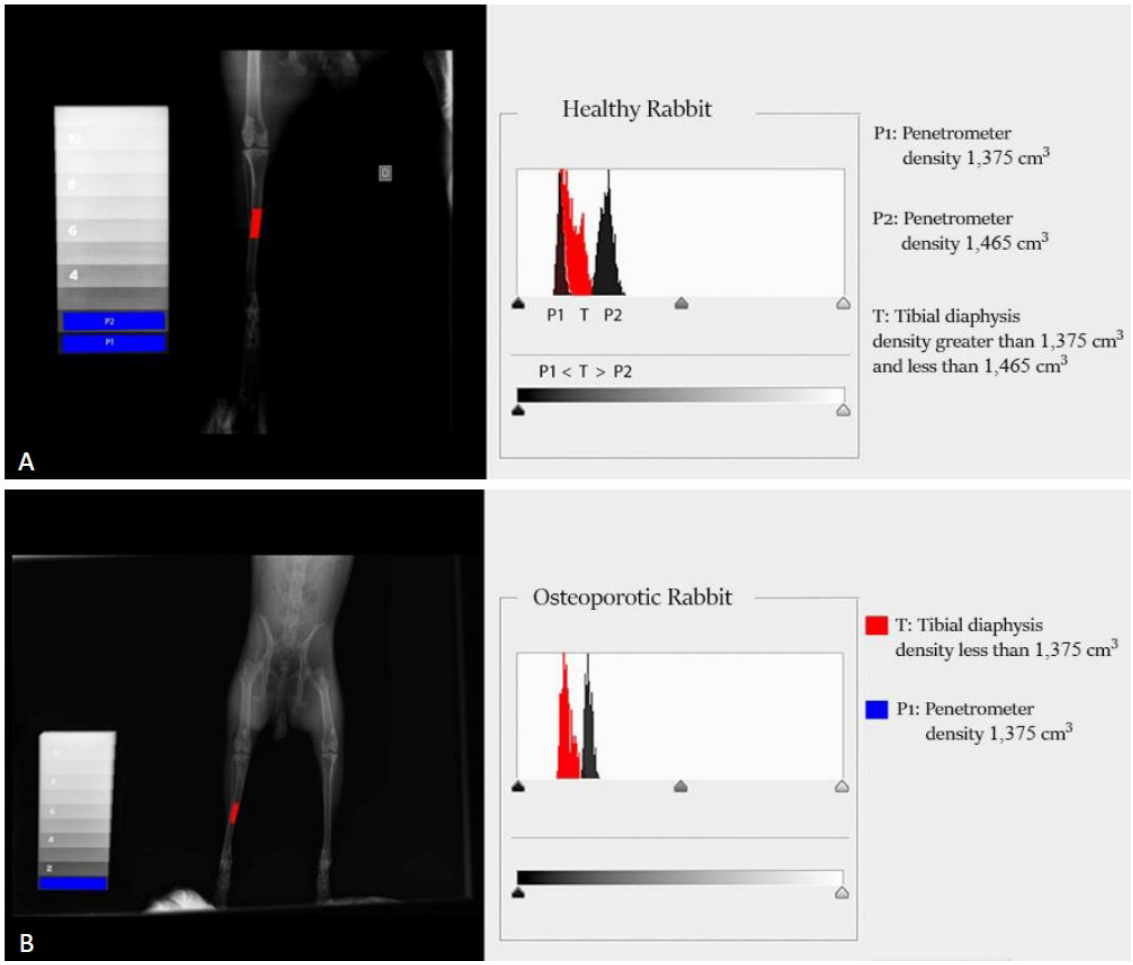

Figure 1 - Radiographic optical densitometry images of the tibia of a rabbit before and after the induction of hypercortisolism and osteoporosis. **A**: Before the induction of the model, the bone density is greater than 1.375cm³ and less than 1.465cm³. **B**: After induction of the model, the bone density is less than 1.375cm³, evidencing loss of bone density.

Table 3 - Radiographic optical densitometry (cm^3) intervals of adult nulliparous rabbits, submitted to ovariosalpingohysterectomy, before and after induction of iatrogenic hypercortisolism and osteoporosis using 11-step aluminum penetrometer.

	Before induction (cm^3)	After induction (cm^3)
Animal 1	1.37<**X**≤1.55	**X** <1.37
Animal 2	1.37< **X**≤1.46	**X** <1.37
Animal 3	1.37< **X**≤1.55	**X** <1.37
Animal 4	1.37< **X**≤1.55	**X** <1.37
Animal 5	1.37< **X**≤1.46	**X** <1.37
Animal 6	1.37< **X**≤1.55	**X** <1.37
Animal 7	1.37< **X**≤1.55	**X** <1.37
Animal 8	1.37< **X**≤1.55	**X** <1.37
Average	1.37< **X**≤1.52	**X** <1.37

The obtained PRP had 82% of the initial platelet volume concentration, but in a volume 10 times lower than the initial one.

The MSC culture with a sterile hydrolyzed collagen sponge fragment identified that the cells adhered to the sponge matrix after 10 days of incubation (Figure 2 A-B) and the average cell viability assessed after removal of the fragment was 95%.

The histological evaluation of the same sponge fragment identified the presence of mononuclear cells adhered to the substrate of the same, with intact nucleus and loosely condensed chromatin (Figure 2C).

Radiographic optical densitometry identified statistically significant differences between treatments evaluated only after 60 days (p≤0.008), with higher average bone density in MSC treated animals. No statistically significant differences were observed between the PRP and ASSO groups (p≤0.88) (Table 4) (Figure 3).

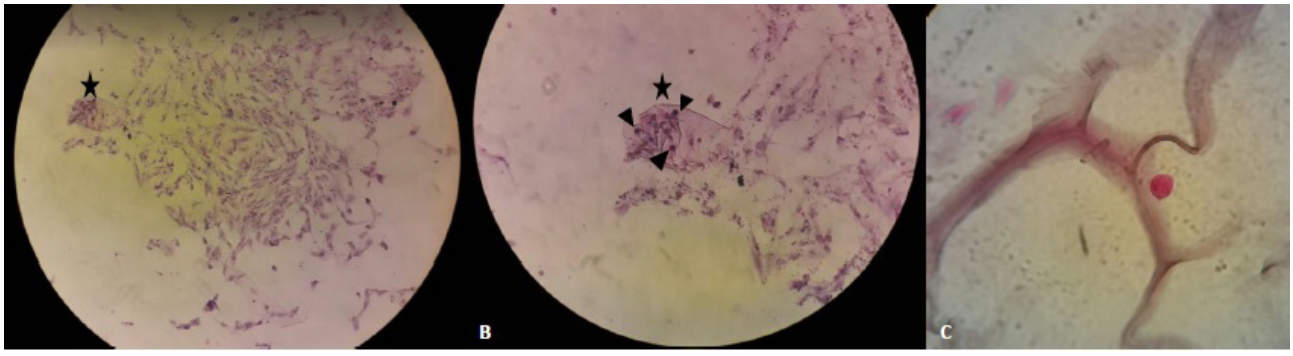

Figure 2 - Interaction between rabbit medullary mesenchymal stem cells and hemostatic sponge of hydrolyzed collagen. **A**: Cells after 10 cultures fixed with 10% buffered paraformoldehyde and stained with May-Grunwald Giemsa, bordering the sponge fragment (★) (x20). **B**: Uniform colony of fibroblast cell morphology with central nucleus and mononuclear cells (◢) on sponge fragment (★) (x40). **C**: Histological cut of the sponge after 10 days of incubation in culture with rabbit medullary mesenchymal stem cells. The presence of a mononuclear cell, of loose chromatin, adhered to the convolutions of the sponge matrix (x40) (Hematoxylin & Eosin) is identified.

Table 4 - Average radiographic optical densitometry (cm^3) intervals of filling of tibial cortical failures of osteoporotic rabbits after 30 and 60 days of treatment with sterile hemostatic hydrolyzed collagen sponge (CTR), mesenchymal stem cells (MSC), platelet rich plasma (PRP) and association (ASSO) between the two.

Treatment	30 days (cm^3)	60 days (cm^3)
CTR	**X** ≤1.37[b]	**X** <1.37[b]
MSC	1.37≤ **X**≤1.46[b]	1.55< **X**≤1.64 [a]
PRP	1.37≤ **X**≤1.46[b]	1.37≤ **X**≤1.55[c]
ASSO	1.37≤ **X**≤1.46[b]	1.37≤ **X**≤1.55[c]

Pairs of average followed by different letters, in the same column, differ from each other by the Dunn test at 1% significance.

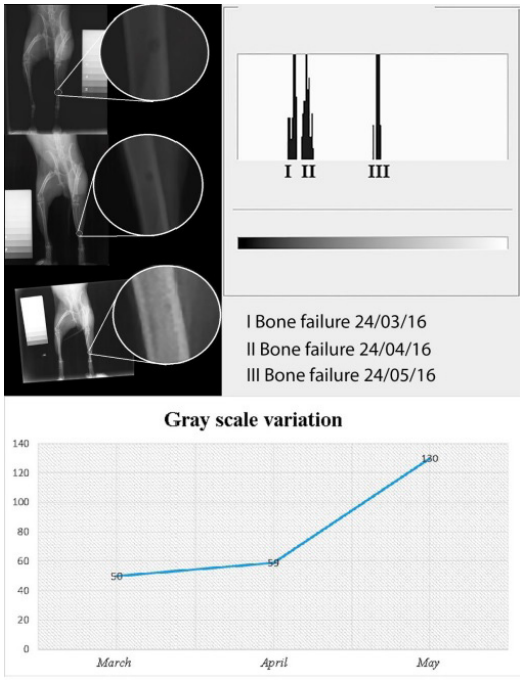

Figure 3 - Radiographic optical densitometric evaluation of a tibial bone failure of a CTM-treated rabbit and the corresponding gray scale variation. **A**: Serial radiographic images over 60 days, showing the maximum radiolucency variation of bone failure with minimal density (I and II) and minimum radiolucency with maximum bone density (III). **B**: Variation of the gray graduation curve, corresponding to bone density, over 60 days. The darkest tone corresponds to black and has a value of 0, representing maximum radiolucency of the bone defect. The lighter tone corresponds to white and has a maximum value of 255, representing minimal radioluscence of bone failure. The curve shows progressive elevation of white tones over time, characterizing the gradual increase of the bone density of the analyzed fault.

Microscopically, after 30 days of treatment, all bone failures of all groups showed bone growth interruption lines, with presence of mature bone composed of osteocytes, organization of trabecular bone tissue without presence of osteoblasts and areas of osteopenia. After 60 days, histopathological differences in the remodeling of bone failures between the treated groups were identified (Figure 4). The CTR group presented histopathological similarities to the groups treated after 30 days, predominating osteocytes in detriment of osteoblasts. The MSC group presented mature and immature bone, failure lines of bone growth, organization of trabecular bone with angiogenesis and presence of active osteoblasts, synthesizing osteoid matrix. The PRP group identified mature bone, failure lines of bone growth, moderate presence of immature bone, predominating osteocytes in the fields evaluated and focal areas of osteopenia and fibrosis. The ASSO group presented microscopic aspects similar to PRP, but with few osteoblasts present in the trabecular bone.

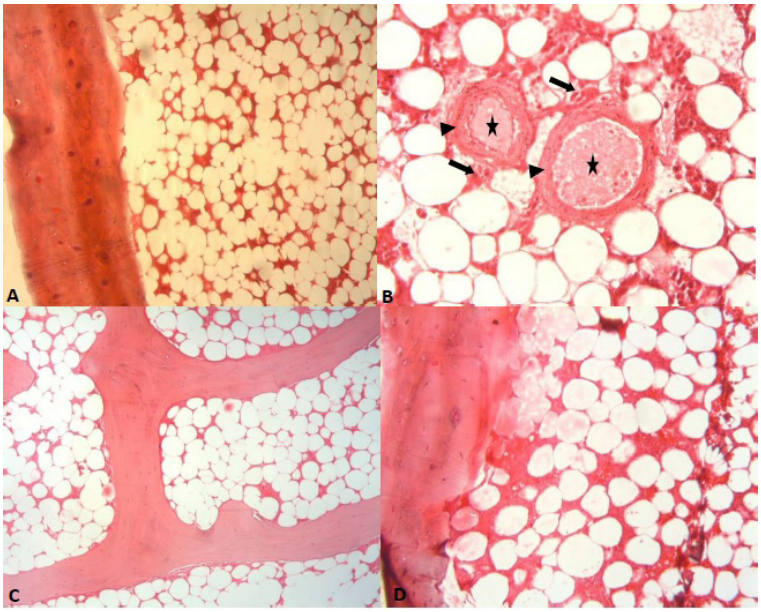

Figure 4 - Photomicrography of tibial bone defects of rabbits with induced osteoporosis after 60 days of treatment with sterile hydrolyzed collagen sponge (CTR), stem cells mesenchymal (CTM) in collagen sponge (EH), platelet-rich plasma in HD (PRP) and association between CTM and PRP in HD. **A**: Group CTR. Border area between discrete bone Compact and marked presence of trabecular bone, without presence of active osteoblasts (x10). **B**: CTM Group. Immature trabecular bone with osteoid tissue organization (►) adjacente to the central vessels (★) And marked presence of active osteoblasts (➡) (x20). **C** and **D**: ASSO and PRP groups, respectively. Compact mature bone and abundant trabecular bone formation, with rare osteoblast (x20) figures.

■ Discussion

Iatrogenic hypercortisolism induced significant changes in serum ionizable calcium concentration, as well as bone density (Figure 1), but with irregular variations in serum phosphorus concentration (Table 2). The average elevation observed in calcium and phosphorus concentrations had already been described by Lanna *et al*.[3] and Romanholi and Salgado[4]. According to these authors, chronic administration of corticosteroids, although in therapeutic doses, may induce iatrogenic secondary hyperparathyroidism to parathyroid hyperplasia. Such condition stimulates the reabsorption of calcium and releases it, along with phosphorus ion to the extracellular medium[4]. However, phosphorus does not circulate in plasma bound to serum proteins, being fully filtered in the glomerulus and easily reabsorbed in the contorted tubules. During osteoporosis, parathyroid hormone binds to the enzyme adenyl cyclase, inhibiting the co-transport of phosphorus in the contorted tubules, inducing phosphaturia and allowing the reabsorbed calcium ions to not be re-incorporated into the bone tissue[3]. Although the concentration of urinary phosphorus in the present study has not been evaluated, it is believed that this condition has occurred, corroborating for the presumption of success in the proposed model.

Radiographic bone densitometry data (Figure 1) (Table 3) demonstrate a marked reduction in the tibia bone density of all rabbits. This technique had already been well described in rabbits[18], rats[19], cats[20], equines[21] and humans[22], among other species. To minimize the possibility of radiographic standardization errors, an 11-step ultra-purified aluminum

penetrometer was used as a densitometric reference, as proposed by Louzada[18]. According to this author, this technique presents high sensitivity, precision, reproducibility, fidelity, easy feasibility and low cost and is widely described by other researchers, especially applied to rabbits with induced osteoporosis[3], which justifies its adoption in the methodology presented in this study.

All the rabbits induced to hypercortisolism and osteoporosis presented average bone densities inferior to 1.37cm^3, having the last step of lower density of the penetrometer as densitometric reference. In this respect, a limitation of the proposed method is identified when a penetrometer of only 11 steps is used, because it is not possible to accurately determine the values below this threshold. Possibly, the adoption of a penetrometer with 21 steps or more would allow us a more accurate evaluation. However, this fact does not obliterate the observation that the association between ovariosalpingohystectomy and corticosteroid administration induces a marked reduction of bone density.

In the present study, the use of a commercial hydrolyzed collagen sponge made from freeze-dried sterile porcine gelatine, as carrier or *scaffold* for MSC and PRP was chosen. This biomaterial was sought because it did not trigger a local inflammatory response, whose degradation time does not interfere in the bone repair process and presents mechanical properties adequate for application in bone failures, as previously described in contemporary studies[23-26].

The in vitro biocompatibility assay between MSC and a fragment of the sponge demonstrated that there was no apparent cytotoxic effect on the cells, since MSC was identified in culture adhered to the fragment, with maintenance of cell viability in 95% (Figure 2 A-B). Analogously, cells adhered to the substrate of the fragment were identified after histological processing, denoting that the substrate matrix provides a favorable environment for cell adhesion (Figure 2c).

The choice of the xenogeneic PRP presentation adopted in the present study contradicts the main scientific observations described[24,26]. According to these authors, xenogeneic PRP has a high immunogenic factor when compared to allogeneic and autogenic presentations. However, being one of the main limitations to the clinical use of PRP, the low yield when compared to the volume of the initial plasma sample[10], especially for infusion in extensive tissue areas, it becomes urgent to search for alternatives that allow obtaining higher volumes of PRP for continuous use. Due to the scarce studies in human and veterinary medicine on the subject, it was proposed the use of PRP obtained from a large animal in the model of osteoporosis of the present research.

The analysis of the effects of treatments on the filling of bone failures allowed us to infer that there is no radiographically evident bone remodeling within 30 days after treatment for all groups evaluated ($p \leq 0.87$). The observed bone density varied between values below 1.375cm^3 and up to 1.465cm^3, corresponding to the last and penultimate step of the penetrometer, respectively. Previous studies have described, in rabbits and mice, the predominant presence of fibrous connective tissue, associated with intense mixed inflammatory infiltration at the site of failure, in the first 30 days after bone failures in healthy or unhealthy patients[13,12]. These authors also used MSC and PRP as treatments for the analyzed bone failures, a fact that corroborates, with the densitometric findings of the present study, suggesting little local bone mineralization.

This hypothesis is supported by histopathological findings after 30 days of treatment. The observed bone growth interruption lines show abrupt discontinuation

of osteoid matrix production and subsequent recovery, as described previously[13,27]. However, in this study, no local inflammatory infiltrate was observed, but only coarse and porous trabecular formation, without osteoblasts. This result suggests low or non-existent osteoid matrix formation and, therefore, likely low structural stability. These observations are consistent with previous descriptions of commonly identified histopathological abnormalities in bone with mineralization deficits, such as osteoporosis[2,5].

It should be emphasized that the histological description of the tibia of healthy rabbits diverges from the histopathological findings in the failures with up to 30 days of treatment[27]. According to these authors, the microscopic structure of the healthy tibia is composed of well-compacted mature bone, with active osteoblasts diffusely distributed at the interface between the compact bone and the abundant trabecular bone, as well as on the surface of the trabeculae, being organized into islands of ossification and in the vicinity of blood vessels.

Diametrically observed at 30 days, significant densitometric differences were identified between treatments after 60 days of observation ($p \leq 0.008$) (Table 4). The CTR group had the lowest bone density when compared to the others. This observation evidences treatment ineffectiveness in inducing consolidation of bone failure. Previous studies have also obtained similar results in rabbits and humans, using hemostatic sponge of hydrolyzed collagen, demonstrating that it does not contribute significantly to bone repair[25].

The MSC group presented the highest densitometric indices, when compared to the other treatments, after 60 days of observation, as determined by the Dunn median test (Table 4). The tibial bone failures of the animals of this group had lower radiopacity than the other treatments ($p \leq 0.008$). The grayscale curve increased progressively from 50 tones, closer to the black color and therefore with lower bone density, to the final value of 130 tones, closer to the white color, evidencing a higher tissue density in the densitometric scale adopted (Figure 3).

The increase in bone density in the MSC group is justified by the histopathological findings (Figure 4). The presence of growth failure lines can be triggered by secondary osteoporosis as suggested in a recent study[2]. It is evident that angiogenesis is evident in the trabecular bone, indicative of the acute phase of bone repair, with osteoid matrix structuring of immature braided osteophyte immediately adjacent to the blood vessels and massive infiltration of active osteoblasts, suggesting that they are responsible for matrix deposition. These characteristics suggest an intensification of the bone repair process, in the remodeling phase, since no inflammatory infiltrate was identified, as described previously[13,27].

Given the osteopenia present in the animals of the present study due to secondary osteoporosis and absence of microscopic observation of an inflammatory cellular component in the flaws evaluated in the MSC group, there is a greater plausibility of differentiation of the MSC in vivo in osteoblastic lineage than the chemotactic stimulus of the same for the attraction of equidistant osteoblasts. Therefore, the massive presence of active osteoblasts and deposited osteoid matrix suggests a higher mineral deposition, which would justify the observed densitometric elevation.

There were no statistically significant differences ($p \leq 0.87$) between the PRP and ASSO groups, to the Dunn test, for radiographic optical densitometry (Table 4).

Histopathological findings suggest the presence of osteopenia in the PRP and ASSO groups, especially in the first group. Characteristics of osteopenia have been described in previous studies, characterized

by the increase of trabecular bone, to the detriment of compact bone and the absence of angiogenesis and active osteoblasts synthesizing osteoid matrix, inducing bone fragility[5,27]. The presence of osteopenia corroborates the densitometric findings of intermediate density, when these groups were compared with the CTR and MSC groups.

The results suggest that PRP contributed positively to repair of bone failure, but less than the group treated with MSC and similar intensity to the ASSO group. Platelets have been described as rich in growth factors and pro-epithelizing cytokines, being activated by contact[13]. In the present study, it is estimated that hydrolyzed collagen sponge as an exogenous factor contributed to the mechanical activation by contact of the platelets present in the PRP, favoring the release of the growth factors immediately to the surgical implantation of sponge fragments in the bone failures.

Contrary to previously mentioned[24,26], no histopathological features were suggested that suggested an increase in bone resorption mediated by immunogenicity by xenogenic PRP. However, the preliminary result is considered and reliable inferences regarding the immune response to xenogeneic PRP are not possible. Further studies are needed to measure pro-inflammatory and anti-inflammatory serum cytokine profiles induced by PRP infusion in bone failures to elucidate such issues. However, the present study demonstrated that xenogenic PRP did not induce elevation of bone resorption.

When in association with MSC (ASSO group), no densitometric or histopathological benefit of the interation was observed (Table 4). Although the ASSO group presented densitometry superior to the CTR group, with lower osteopenia than the same, the results obtained were inferior when compared to the exclusive treatment with allogeneic MSC. Since the same cell line was used, the lowest contribution of the ASSO group to the possible negative interaction with xenogenic PRP is attributed. The present study raises a relevant question about the interaction of MSCs and xenogeneic profiles of cytokines and growth factors, which should be elucidated in later research to improve the model proposed here.

■ Conclusions

The sterile hemostatic hydrolyzed collagen sponge presented favorable biocompatibility with the allogeneic mesenchymal stem cells used, allowing them to be adhered and preserving their viability.

The treatment of bone failures with allogeneic mesenchymal stem cells carried in a fragment of sterile hemostatic sponge induced a higher increase in radiographic optical densitometry with greater microscopic deposition of the osteoid matrix, suggesting an intensification of the bone repair process, in the remodeling phase, when compared to the other treatments.

■ References

1. Patrício JP, Oliveira P, Faria MT, Pérez MB, Pereira J. Osteoporose induzida por corticóides. Arq Med. 2006;20(5-6):173-8. PMID: 754375.
2. Silva ACV, Rosa MI, Fernandes B, Lumertz S, Diniz RM, Damiani MEFR. Fatores associados à osteopenia e osteoporose em mulheres submetidas à densitometria óssea. Rev Bras Reumatol. 2015;55(3):223–8. doi: 10.1016/j.rbr.2014.08.012.
3. Lanna CMM, Montenegro Jr. RM, Paula FJA. Fisiopatologia da osteoporose induzida por glicocorticoide. Arq Bras Endocrinol Metab. 2003;47(1):9-18. PMID: 565878.
4. Romanholi DJPC, Salgado LR. Síndrome de cushing exógena e retirada de glicocorticoides. Arq Bras Endocrinol Metab. 2007;51(8):1280-92. PMID: 471744.
5. Amadei SU, Silveira VAS, Pereira AC, Carvalho YR, Rocha RF. A influência da deficiência

estrogênica no processo de remodelação e reparação óssea. J Bras Patol Med Lab. 2006;42(1):5-12. PMID: 545868.
6. Kowalski SC, Sjenzfeld VL, Ferraz MB. Utilização de recursos e custos em osteoporose. Rev Assoc Med. Bras. 2001;47(4):352-7. PMID: 656755.
7. Pozzi S, Marcheselli R, Sacchi S, Baldini L, Angrilli F, Pennese E, Quarta G, Stelitano C, Caparotti G, Luminari S, Musto P, Natale D, Broglia C, Cuoghi A, Dini D, Di Tonno P, Leonardi G, Pianezze G, Pitini V, Polimeno G, Ponchio L, Masini L, Musso M, Spriano M, Pollastri G. Biphosphonate-associated osteonecrosis of the jaw: a review of 35 cases and an evaluation of its frequence in multiple myeloma patients. Leuk Lynphoma. 2007;48(1):56-64. doi: 10.1080/10428190600977690.
8. Khajuria DK, Razdan R, Mahapatra DR. Medicamentos para o tratamento da osteoporose: revisão. Rev Bras Reumatol. 2011;51(4):365-82. PMID: 767854.
9. Argôlo Neto NM, Feitosa MLT, Sousa SS, Fernandes PB, Pessoa GT, Bezerra DO, Almeida HM, Carvalho YKP, Rocha AR, Silva LMC, Carvalho MAM. Isolation, expansion, differentiation and growth kinetics essay in mesenchymal stem cells culture from the bone marrow of collared peccaries (Tayassu tajacu). Acta Sci Vet. 2016;44:1-11. PMID: 586647.
10. Carvalho YKP, Argôlo Neto NM, Ambrósio CE, Oliveira LJ, Rocha AR, Silva JB, Carvalho AAM, Alves FR. Isolation, expansion and differentiation of cellular progenitors obtained from dental pulp of agouti (Dasyprocta prymnolopha Wagler, 1831). Pesq Vet Bras. 2015;35(6):590-8. doi: 10.1590/S0100-736X2015000600018.
11. Zamprogno H. Células tronco esqueléticas para o tratamento da não união de fraturas. Acta Sci Vet. 2007;35:289-90. PMID: 587456.
12. Del Carlo RJ, Monteiro BS, Silva PSA, Argolo N, Serakides R. Aspectos microscópicos da reparação mediada por plasma rico em plaquetas e autoenxerto esponjoso em falhas ósseas experimentais no crânio de coelhos. Vet Zootec. 2009;16(1):152-60. PMID: 567454.
13. Monteiro BS, Argolo Neto NM, Del Carlo RJ. Células-tronco mesenquimais. Ciênc Rural. 2010;40(1):238-45. PMID: 467455.
14. Raghoebar GM, Schortinghuis J, Liem RSB, Ruben JL, van Der Wal JE, Vissink A. Does platelet-rich plasma promote remodeling of autologous bone grafts used for augmentation of the maxillary sinus floor? Clin Oral Implants Res. 2005;16(3):349-56. doi: 10.1111/j.1600-0501.2005.01115.x.
15. Bueno CM, Cerejo AS, Miguel MP, Franco LG, Honsho CS. Utilização do 2-octil-cianoacrilato na ovariectomia de coelhas, comparativamente ao fio de náilon: análise de tempo e alterações macroscópicas. E Biosfera. 2012;8(15):1657-71. PMID: 765457.
16. Argôlo Neto NM, Del Carlo RJ, Monteiro BS, Nardi NB, Chagastelles PC, de Brito AFS, Reis AMS. Role of autologous mesenchymal stem cells associated with platelet-rich plasma on healing of cutaneous wounds in diabetic mice. Clin Exp Dermatol. 2012;37(5):544-53. doi: 10.1111/j.1365-2230.2011.04304.x.
17. Cunha AP., Bello ACPP, Leite RC, Melo MM, Braz GF, Ribeiro ACCL, Oliveira PR. Avaliação de parâmetros clínicos e hematológicos de eqüinos submetidos a um programa de controle estratégico de Amblyomma cajennense (Fabricius, 1787) (Acari: Ixodidae). Arq Bras Med Vet Zootec. 2008;60(1):113-20. PMID: 483266.
18. Louzada MJQ. Densitometria óptica radiográfica na mensuração da densidade mineral óssea de coelhos em crescimento. Ars Vet. 2002;18(2):107-10. PMID: 538367.
19. Silva ARS, Ribeiro ACP, Salzedas LMP, Soubhia AMP, Sundefeld MLMM. Análise da densidade óssea radiográfica de ratos submetidos ao alcoolismo crônico utilizando imagem digital. Rev Odonto Ciênc. 2007;22(55):77-81. PMDI: 765365.
20. Rahal SC, Mortari AC, Caporali EHG, Vulcano LC, Santos FAM, Takahira RK, Crocci AJ. Densitometria óptica radiográfica na avaliação do hiperparatireoidismo secundário nutricional induzido em gatos jovens. Cienc Rural. 2002;32(3):421-5. PMID: 395345.
21. Godoy CLB, Vulcano LC, Santos FAM, Soares JCM. Valores normais da densidade mineral óssea do acessório do carpo em equinos da raça brasileiro de hipismo (BH) determinados por meio da densitometria óptica em imagem radiográfica. Cienc Rural. 2005;35(3):607-10. PMID: 649643.

22. Canali GD, Takahashi CM, Mello AS, Costa MB, Souza PHC, Tolazzi AL, Westphalen VPD, Westphalen FH. Estudo comparativo da densidade óptica óssea obtida em radiografias panorâmicas e da densitometria óssea em mulheres histerectomizadas e não histerectomizadas. Rev Fac Odontol UPF. 2011;16(2):149-53. PMID: 873678.
23. Oliveira GK, Raiser AG, Olsson D, Salbego FZ, Martins DB, Dezengrine R, Santos Júnior EB, Rappeti J, Trindade LB, Tognoli GK, Pippi NL, Sausen L. Células-tronco mononucleares autólogas e proteína óssea morfogenética na cicatrização de defeitos tibiais experimentalmente induzidos em cães. Arq Bras Med Vet Zootec. 2010;62(1):72-9. PMID: 543071.
24. Yamada ALM, Alvarenga ML, Brandão JS, Watanabe MJ, Rodrigues CA, Hussni, CA, Alves AL. Arcabouço de PRP-gel associado a células tronco mesenquimais: uso em lesões condrais em modelo experimental equino. Pesq Vet Bras. 2016;36(6):461-7. doi: 10.1590/S0100-736X2016000600001.
25. Gabrielli MAC, Hochuli-Vieira E, Paleari AG, Cerri P. S., Klüppel LE. Avaliação histológica de agentes hemostáticos implantados em mandíbulas de coelhos. Rev Cir Traumatol Bucomaxilofac. 2009;9(2):97-106. PMID: 654987.
26. Moshiri A, Oryan A. Role of platelet rich plasma in soft and hard connective tissue healing: an evidence based review from basic to clinical application. Hard Tissue. 2013;2(1):6. PMID: 685437.
27. Moreira R, Dória RG, Camargo LM, Santos MD, Minto BW, De Nardi AB, Ambrósio CE, Freitas SH. Aspecto radiológico e macroscópico de matriz óssea mineralizada heteróloga fragmentada e polimetilmetacrilato autoclavados em falha óssea de tíbia de coelho. Pesq Vet Bras. 2014;34(2):173-8. doi: 10.1590/S0100-736X2014000200013.

■ Acknowledgement

To University Veterinary Hospital, UFPI.

Correspondence:
Napoleão Martins Argôlo Neto
Campus Ministro Petrônio Portela
Centro de Ciências Agrárias
64049550 Teresina – PI Brasil
Tel.: (55 86)99938-1386
argolo_napoleao@ufpi.edu.br

Received: May 12, 2017
Review: July 14, 2017
Accepted: Aug 18, 2017

Conflict of interest: none
Financial sources: CAPES

[1]Research performed at Integrated Nucleus of Morphology and Research with Stem Cell (NUPCelt), Agrarian's Sciences Center, Universidade Federal do Piauí (UFPI), Teresina-PI, Brazil.